Molecular basis of flowering under natural long-day conditions in Arabidopsis

Title: Molecular basis of flowering under natural long-day conditions in *Arabidopsis*

Authors:

Young Hun Song[1,2]*, Akane Kubota[1]*, Michael S. Kwon[1], Michael, F. Covington[3], Nayoung Lee[1], Ella, R. Taagen[1], Dianne Laboy Cintrón[1], Dae Yeon Hwang[2], Reiko Akiyama[4], Sarah, K. Hodge[5], He Huang[6], Nhu H. Nguyen[1], Dmitri, A. Nusinow[6], Andrew, J. Millar[5], Kentaro K. Shimizu[4,7], and Takato Imaizumi[1]

Affiliations:

[1]Department of Biology, University of Washington, Seattle, WA, 98195, USA.

[2]Department of Life Sciences, Ajou University, Suwon, 443-749, Korea.

[3]Amaryllis Nucleics, Oakland, CA, 94609, USA.

[4]Department of Evolutionary Biology and Environmental Studies, University of Zürich, 8057 Zürich, Switzerland.

[5]School of Biological Sciences and SynthSys, University of Edinburgh, Edinburgh, EH9 3BF, UK

[6]Donald Danforth Plant Science Center, St. Louis, MO, 63132, USA.

[7]Kihara Institute for Biological Research, Yokohama City University, Yokohama, Kanagawa, 244-0813, Japan

* These authors contributed equally to this work.

Abstract: Plants sense light and temperature changes to regulate flowering time. Here we show that the expression of the florigen gene, *FLOWERING LOCUS T* (*FT*), peaks in the morning during spring, a different pattern than we observe in the lab. Providing our lab growth conditions with a red/far-red light ratio similar to open field conditions and daily temperature oscillation is sufficient to mimic the *FT* expression and flowering time in natural long days. Under the adjusted growth conditions, key light signaling components, such as phytochrome A (phyA) and EARLY FLOWERING 3 (ELF3), play important roles in morning *FT* expression. These conditions stabilize CONSTANS (CO) protein, a major *FT* activator, in the morning, which is likely a critical mechanism for photoperiodic flowering in nature. Refining the parameters of our standard growth conditions to more precisely mimic plant responses in nature can provide a powerful method for improving our understanding of seasonal response.

Main Text:

Many plants and animals utilize day-length (=photoperiod) information to control various seasonal responses for survival and reproduction, as the changes in photoperiod occur in a predictable manner from year to year. Among the seasonal responses, flowering regulation in *Arabidopsis* is the most characterized photoperiodic response at the molecular level[1, 2]. Photoperiod and temperature information is processed through circadian clock-dependent mechanisms to ultimately induce the expression of the florigen gene, *FT*, around dusk in long days (LD)[3, 4, 5]. This LD specific *FT* induction occurs in phloem companion cells in leaves. Once FT protein is synthesized in LD, FT protein is transferred from the leaves to the shoot apical meristem to trigger the cascade of events that initiates the transition from vegetative to reproductive development[6, 7]. Many components in the *Arabidopsis* photoperiodic pathway are highly conserved in angiosperms (including major crops such as rice, wheat, barley, and

potato) to regulate seasonal responses. For instance, genes identified through quantitative trait locus (QTL) analyses on flowering time, yield, or other domestication traits (often tied with loss/reduction of photoperiod sensitivity) in many crops frequently turned out to be homologs of the *Arabidopsis* photoperiodic flowering components[8]. The photoperiodic sensing mechanism originally characterized in *Arabidopsis* was found to already exist in bryophytes to regulate photoperiodic reproductive development[9]. This indicates that incorporating photoperiodic information into developmental regulation has been important for land plant survival. Thus far, *Arabidopsis* research has been instrumental in not only identifying the components involved in photoperiodic flowering, but also understanding how these components function in this pathway under well-controlled lab settings. However, it remains unknown whether the current model of photoperiodic flowering regulation can recapitulate the major mechanisms that regulate seasonal flowering in complicated natural LD environments. Here we show the presence of a previously uncharacterized regulation of florigen induction in *Arabidopsis* plants grown under natural LD conditions, and our subsequent attempt to elucidate its regulatory mechanism using lab growth conditions optimized to plant responses in nature.

Results

Flowering regulation under natural LD conditions

Light (both day length and light quality) and temperature are major environmental parameters that control flowering time[3, 5, 10]. The outside day length and temperature conditions of the summer solstice in Seattle, WA, USA, (47°36′N; day length, 15 hours 59 min; average high temperature from 1971 to 2000, 21.1 °C) were similar to our lab LD conditions (16 hours, constant 22 °C). In addition, ecological studies showed that summer annuals of wild *Arabidopsis* plants grown in similar latitudes to Seattle germinate and flower within a roughly one month period between March and July in both Europe and North

America (the actual timing of flowering varies by location)[11, 12, 13, 14, 15, 16, 17, 18]. Therefore, we tested how accurately photoperiodic flowering regulation that occurs in controlled lab environments can represent flowering regulation under similar natural LD conditions in spring.

We grew wild-type (WT: Col-0) plants outside in Seattle in June and harvested them around the summer solstice (Fig. 1a and Supplementary Fig. 1). We analyzed the expression of genes important for photoperiodic flowering regulation: circadian clock genes, clock outputs of photoperiodic flowering genes, core photoperiodic flowering genes, such as *CONSTANS* (*CO*), and *FLOWERING LOCUS T* (*FT*) genes, and floral repressor genes (Fig. 1b, c and Supplementary Fig. 2)[5, 19]. The expression patterns of six circadian clock genes, clock output flowering genes, and floral repressor genes were relatively similar to those already described in the lab-grown samples (Supplementary Fig. 2)[20, 21, 22, 23]. In addition, the night-peaking *CO* expression profile was similar to the one in lab LD with cooler nights (Fig. 1b)[23]. These results indicate that simplified lab conditions recapitulate the natural gene expression profiles of those genes. However, in the plants grown outside, *FT* showed a bimodal expression pattern with peaks in the morning and around dusk (Fig. 1c), which clearly differed from the typical *FT* pattern peaking near dusk in lab LD[21, 24]. We also observed a similar bimodal expression pattern in *TWIN SISTER OF FT* (*TSF*), a related florigen gene (Supplementary Fig. 2l)[24].

Since *FT* levels strongly correlate with flowering time[23, 25], we analyzed the flowering time of Col-0 plants grown under natural LD conditions. During the last five years, even though temperatures around the summer solstice varied (Supplementary Fig. 1), Col-0 plants all flowered at similar developmental times, and earlier than the plants grown in lab LD (Fig. 1d). In addition, we repeatedly observed similar *CO* and *FT* expression patterns in samples harvested around the last five summer solstices (Fig. 1b, c, e-g and Supplementary Fig. 3 and

5). We also grew other accessions, such as a common lab accession, L*er,* and another WT accession, Vancouver-0 (Van-0) in natural LD. Van-0 was isolated from the location closest to Seattle (Vancouver, BC, Canada; 49°15′N). We speculated that Van-0 is adapted to an environment similar to Seattle. Both accessions flowered earlier than Col-0 in lab LD, even slightly earlier in natural LD (Fig. 1d), and showed similar bimodal *FT* expression patterns under the conditions (Supplementary Fig. 4).

We also analyzed the phenotypes of some non-transgenic alleles of photoperiodic flowering mutants, such as *flavin-binding, kelch repeat, f-box 1 (fkf1*) and *gigantea* (*gi-2*), in natural LD. The flowering time of these late-flowering mutants was significantly earlier than the same mutants grown in lab LD (Fig. 1d). The *fkf1* mutant flowered at almost the same time as Col-0 plants in natural LD, suggesting that some regulation that takes place outside but not in the lab may trigger earlier flowering in the *fkf1* mutant. When we analyzed *FT* expression patterns in *fkf1* and *gi-2* grown in natural LD, the *gi-2* mutant lost *FT* expression as expected[26], but the morning *FT* expression was clearly observed in *fkf1* (Fig. 1e). *FT* is not induced in *fkf1* in lab LD[21], resulting in a strong late flowering. These results suggest that morning *FT* expression in *fkf1* is likely the cause of the early flowering phenotype of *fkf1* in natural LD, and also that there must be a morning-specific mechanism of *FT* induction, in which FKF1 might not be heavily involved.

As our results suggested a functional contribution of morning *FT* expression on flowering time in natural LD, we analyzed the expression patterns of *FT* in samples grown in different times in spring (April, May, and June), which is the growth season of summer annuals in Europe. Summer annuals coexist with winter annuals in natural field conditions and flower at some time in spring, especially at relatively lower latitudes in European countries (as well as at higher latitudes in the USA)[11, 12, 13, 14, 15, 17]. In Seattle, the days are already lengthening in April (approximately 14 hours); however, the ambient temperature in

April was colder than in May and June (Supplementary Fig. 1). Col-0 plants flowered later in April than in May and June (Fig. 1h). In all samples grown during spring in the last two years, *FT* peaked in the morning with different levels (lower in April than in May and June) without changing *CO* patterns (Fig. 1f and Supplementary Fig. 5).

Next, we tested whether the *FT* morning peak is observed in two native locations of *Arabidopsis*. We grew Col-0 plants in Zürich (47°37'N, similar latitude to Seattle), and in Edinburgh, (55°57'N, higher latitude than Seattle) in June around the summer solstice. Although the temperatures (and day length in Edinburgh) were different than in Seattle (Supplementary Fig. 6), Col-0 plants grown in both locations flowered at a similar time to the ones grown in Seattle (Fig. 1h). Both samples also showed the morning expression of *FT*, although the afternoon *FT* expression levels differed (Fig. 1g and Supplementary Fig. 7). Taken together, these results indicate that WT plants grown in natural LD during spring induce *FT* in the morning and possibly around dusk to induce early flowering.

Reconstitution of lab growth conditions that reflect natural conditions for flowering

Our results obtained from plants grown outside in spring (=natural LD) demonstrated that our current lab LD conditions are not sufficient to reproduce all important flowering regulation. To more precisely study these mechanisms, we adjusted our current growth conditions using *FT* expression patterns as a proxy for the flowering time regulation in nature. These adjusted growth conditions enabled us to continue to utilize our rich array of transgenic resources to more accurately investigate the molecular mechanisms underlying seasonal flowering responses.

We first hypothesized that the progressive daily oscillation of light intensity might alter the *FT* pattern, compared to step changes (=light on/off) under lab conditions. We tested the effect of light intensity changes on *FT* expression and found that they did not drastically alter the *FT* pattern (or *CO* and *TSF*) (Supplementary Fig. 8a-e), indicating that light on/off

150 conditions might be sufficient. Daily temperature changes affect *FT* expression patterns[23, 27].
151 Therefore, we analyzed the effect of daily temperature fluctuation on *FT* expression. When
152 Col-0 plants were grown in lab LD with daily temperature oscillations based on the average
153 changes that occurred around the summer solstice (Supplementary Fig. 8f, g), *CO* was
154 strongly induced at the end of the night (Supplementary Fig. 8h). The afternoon *FT*
155 expression levels (but not the *TSF* levels) were severely repressed by daily temperature
156 changes (Supplementary Fig. 8i, j). These results suggest that temperature oscillation is not
157 enough to induce *FT* in the morning, although it can repress *FT* in the afternoon.
158 The red to far-red (R/FR) ratio in an open field (including our outside conditions) is
159 approximately 1 (ref 28), but it varies from approximately 2 (our lab conditions) to 13 (ref
160 28) under fluorescent lamps. Plant shade conditions (=very low R/FR ratios) highly induce
161 the expression of *FT* even in the morning[29, 30]. We wondered whether the morning *FT* peak
162 could be induced under R/FR ratio=1 conditions. To test this, we supplemented our
163 fluorescent lamps (R/FR=2) with dim FR LEDs to adjust the R/FR ratio to 1 (Supplementary
164 Fig. 9a). Merely adjusting the R/FR ratio from 2 to 1 was sufficient to induce *FT* (and *TSF*)
165 in the morning, without affecting *CO* expression patterns (Fig. 2a and Supplementary Fig. 9b,
166 c). Under these conditions (named LD+FR), the levels of both morning and afternoon *FT*
167 levels were higher than in lab LD (Fig. 2a). However, the afternoon *FT* peak was still slightly
168 higher than the morning peak, different from the *FT* patterns in natural LD.
169 We also tested whether R/FR=1 induces *FT* in the morning independent of
170 photoperiod changes. We analyzed *FT* expression in short days (SD) with R/FR=1 (SD+FR).
171 *FT* was not induced in SD+FR, similar to regular SD (Supplementary Fig. 10), implying that
172 the morning induction of *FT* under LD+FR conditions is long-day specific.
173 As temperature oscillation reduced afternoon *FT* levels (Supplementary Fig. 8i), we
174 hypothesized that combining the R/FR=1 conditions with daily temperature change may

cause a similar *FT* pattern to that observed outside. Incorporating these two parameters in the simplified lab conditions was sufficient to generate similar *FT* expression patterns (and *CO* and *TSF*) to that observed in nature (Fig. 2b and Supplementary Fig. 11). It has been proposed that the afternoon expression of *CO* is important for *FT* induction in LD[1]. A comparison of the *CO* profiles in the samples grown in natural LD, lab LD and LD+FR+temp conditions showed that the *CO* levels differed most around the dawn between outside/LD+FR+temp- and LD-grown samples without changing the afternoon expression of *CO* (Supplementary Fig. 11a).

After we successfully established the modified lab LD conditions (LD+FR+temp) under which *FT* expression patterns resemble those in natural LD, we analyzed the flowering time of WT accessions and photoperiodic mutants including *co*, *ft*, *ft tsf* and *fkf1* under these conditions. Under the LD+FR+temp conditions, similar to the natural LD conditions, WT plants and *fkf1* alleles flowered earlier than those grown in lab LD (Fig. 2c). In addition, the *FT* expression profile in *fkf1-2* was similar to that in *fkf1* grown in natural LD (Supplementary Fig. 12), validating that the simplified LD+FR+temp conditions captured the major environmental parameters to recreate the *FT* expression patterns and flowering time responses of the plants grown in natural LD. Importantly, the *co*, *ft* single and *ft tsf* double mutants still showed a similar late flowering phenotype under all experimental conditions (Fig. 2c). In addition, the *ft-1 tsf-1* double mutants flowered later than the *ft-1* single mutant (Fig. 2c), indicating that changes in the expression patterns of both *FT* and *TSF* may contribute to flowering time in LD+FR+temp. Taken together, these results indicate that the core components (CO and FT) in the photoperiodic pathway still determine flowering time in LD+FR+temp.

We also analyzed whether the LD+FR+temp conditions changed the spatial expression patterns of *FT* to induce its morning peak. The tissue-specific GUS activity

patterns in the *FT:GUS* plants were similar in LD, LD+FR, and LD+FR+temp (Fig. 2d and Supplementary Fig. 13), indicating that the adjustment of the R/FR ratio and temperature mainly affected the temporal expression pattern of *FT*.

To explore the similarities between LD+FR+temp and natural LD conditions on a whole transcriptome scale, we performed RNA-sequencing analysis using WT plants grown in lab LD, LD+FR+temp, and two years (2013 and 2014) of natural LD conditions outside. The samples were harvested at Zeitgeber time 4 (ZT: time after light onset) when morning *FT* peaks. Compared with lab LD conditions, 57 genes were consistently upregulated in the morning in two different years of natural LD and LD+FR+temp conditions (Fig. 3a and Supplementary Table 1). GO term enrichment analysis showed that genes involved in light (UV-B, FR, and R) responses were enriched (Fig. 3a and Supplementary Table 1). Among these 57 genes, only four, including *FT* and *TSF*, were identified as flowering genes, based on FLOR-ID[31] (Fig. 3b). In the downregulated genes common among the three conditions compared with the lab LD condition, environmental stress-related genes were enriched (Supplementary Fig. 14 and Supplementary Table 1). However, there were no downregulated overlapping flowering genes among the three conditions (Supplementary Fig. 14). These results indicate that *FT* and *TSF* induction levels might be the major difference important for flowering time regulation between LD and LD+FR+temp as well as natural LD conditions.

Flowering time is a critical adaptive trait within WT accessions[32]. Our data showed that the generation of the *FT* morning peak was closely related to the early flowering phenotypes in natural LD (Fig. 1c-h). We asked whether this mechanism is widely conserved in WT accessions. To test this, we compared *FT* levels between morning and evening among 20 summer annual accessions[33] originating from different latitudes (Supplementary Fig. 15a) grown in lab LD and LD+FR+temp. In LD, *FT* levels in all accessions were significantly higher in the afternoon than in the morning (Fig. 3c and Supplementary Fig. 15b). However,

in LD+FR+temp, the differences in *FT* levels between morning and evening were much reduced (Fig. 3c and Supplementary Fig. 15c). We did not observe any clear correlations between original latitudes and *FT* patterns. These results suggest that the mechanisms that induce morning *FT* expression in LD+FR+temp are largely conserved across *Arabidopsis* accessions.

Components important for flowering time regulation in nature

As our LD+FR+temp conditions reproduced similar *FT* expression profiles to those in natural LD (Fig. 2b), we next investigated whether any known components in the flowering and light signaling pathways are involved in the regulation of morning *FT* expression. Because CO is a chief activator of *FT*[1], we first analyzed *FT* expression in the *co* mutant. *FT* levels in the *co* mutant were very low throughout the day in LD+FR+temp, LD, and LD+FR (Fig. 4a-c), implying that CO function is essential for *FT* induction even under conditions more similar to the natural environment. We then analyzed *FT* expression patterns in photoreceptor and light signaling mutants, circadian clock mutants, and mutants in the ambient temperature flowering pathway in LD+FR+temp (Fig. 4a-f and Supplementary Fig. 16)[1, 5, 19]. Compared with WT plants, *FT* expression in the morning was specifically reduced in the *phytochrome A* (*phyA*) mutant (*phyA-211*) in LD+FR+temp (Fig. 4a), indicating that phyA signaling is important for induction of *FT* in nature. This phenotype was also pronounced in LD+FR (Fig. 4b, c). As increasing FR light intensity induced *FT* in the morning (Fig. 2a), the involvement of the photoreceptor for FR high irradiance response (=phyA)[34] in this novel regulation is quite reasonable. This prompted us to analyze the flowering phenotype of the *phyA* mutant in natural LD and LD+FR+temp conditions. To grow the *phyA* mutant outside, we utilized non-transgenic *phyA-201* allele (L*er* background), since *phyA-211* possesses a transgene[35]. *phyA-201* flowered later than the parental L*er* plants outside (Supplementary Fig. 17a). Previous studies posited that a certain amount of FR light

is required to observe phyA-dependent effects on flowering, as *phyA* mutants only showed a late flowering phenotype in LD with lower R/FR ratio in the afternoon (=SD+8 hour extension of incandescent light irradiation) or in continuous FR light conditions[10, 36, 37]. In LD+FR+temp conditions, both *phyA-201* and *phyA-211* flowered later than their parental accessions (Supplementary Fig. 17a). These results indicate that both natural LD and LD+FR+temp conditions (R/FR=1) contain enough FR light to observe the phyA contribution to flowering induction. We also analyzed *FT* expression in *phyA-201*, and found that *FT* levels were lower in both morning and afternoon than L*er* plants (Supplementary Fig. 17b, c). This result indicates that, although phyA is clearly involved in the induction of the morning peak of *FT*, its contribution to the afternoon expression of *FT* may differ in either different backgrounds and/or alleles. We further assessed the significance of the phyA signaling using the *far-red elongated hypocotyl 1* (*fhy1*) *fhy1-like* (*fhl*) mutant (Col-0 background) in which phyA signaling is severely attenuated due to impairment of phyA nuclear transport[38]. Although the phenotype was weaker than the *phyA-211* mutant, *fhy1 fhl* also showed a reduction in morning *FT* expression in LD+FR+temp (Supplementary Fig. 16a, b). This result further supports the notion that phyA signaling is involved in flowering regulation through inducing *FT* in natural LD.

phyA functionally antagonizes phyB in flowering[39, 40]. In *phyB* mutant, *FT* levels were higher than in WT plants in LD+FR+temp (Fig. 4d). In *early flowering 3* (*elf3*), which is a phenocopy of the *phyB* mutants[41], *FT* levels were even higher than in the *phyB* mutant (Fig. 4d-f). The difference between *phyB* and *elf3* mutants was more pronounced in LD and LD+FR (Fig. 4d-f). These results suggest that ELF3 may regulate not only phyB signaling but also other signaling pathways important for *FT* induction.

Despite being downstream signaling components of phyB and ELF3[42, 43], PHYTOCHROME INTERACTING FACTOR 1 (PIF1), PIF3, PIF4, and PIF5 might not be

important for *FT* induction in LD+FR+temp, as *FT* profiles in the *pif1 pif3 pif4 pif5* (*pifq*) mutant resembled that in WT (Supplementary Fig. 16c, d). The *FT* levels in both *constitutive photomorphogenic 1* (*cop1*) and the *suppressor of phyA-105 1* (*spa1*) *spa3 spa4* triple mutants were higher without changing *CO* mRNA patterns (Supplementary Fig. 16c, d). As COP1 and SPAs directly control CO protein degradation[44, 45], this indicates that CO protein stability regulation is still important in LD+FR+temp. In the *cryptochrome 1* (*cry1*) *cry2* double mutant, *FT* expression occurred just in the morning, which is similar to the *fkf1* mutants (Supplementary Fig. 12 and 16e, f). In addition, the *CO* levels in *cry1cry2* at ZT1 is higher than that in the WT plants, indicating that both CRY proteins may also regulate *CO* in the morning in LD+FR+temp conditions. The results of *FT* expression in the *cry1 cry2* mutant prompted us to analyze the flowering phenotype of the mutant in LD+FR+temp. The *cry1 cry2* mutant flowered significantly earlier in LD+FR+temp than in LD (Supplementary Fig. 18), which resembles the flowering phenotypes of *fkf1* mutants. This result further indicates that the morning expression of *FT* contributes to flowering time regulation. These results suggest that these two classes of blue-light photoreceptors are important for the afternoon *FT* expression.

Circadian clock components often regulate *FT* expression in LD[1]. *FT* expression levels were depressed in both *gi* and *pseudo response regulator7* (*prr7*) *prr9* mutants in LD+FR+temp (Supplementary Fig. 16e-h). In the *circadian clock associated 1* (*cca1*) *late elongated hypocotyl* (*lhy*) double mutant, *FT* expression levels during the afternoon were strongly increased in LD+FR+temp (Supplementary Fig. 16g, h). Based on these mutant phenotypes, our results suggest that *GI* and *PSEUDO RESPONSE REGULATOR*s (*PRR*s) are important for the induction of *FT* throughout the day[26, 46], while morning clock genes, CCA1 and LHY, strongly repressed *FT* mainly in the afternoon[1, 47].

In the ambient temperature pathway mutants, such as *short vegetative phase* (*svp*), *svp flowering locus m* (*flm*) *flowering locus c* (*flc*), and *high expression of osmotically responsive genes 1* (*hos1*)[33, 48], the difference in morning *FT* levels looked greater than that in the afternoon (Supplementary Fig. 16i, j). This could be due to lower temperatures in the morning, which activate the ambient temperature pathway. In summary, based on our results, several known components are involved in morning *FT* expression regulation.

To further investigate the mechanisms of morning *FT* induction, we decided to study possible interactions between phyA and ELF3. Our results showed that phyA functions as an *FT* activator, while ELF3 is a strong *FT* repressor in the morning in LD+FR+temp (Fig. 4a, d). In addition, phyA was identified as one of the proteins co-immunoprecipitated with ELF3, indicating that phyA and ELF3 may exist in the same protein complex[49].

First, as *FT* levels are highly increased under lower R/FR ratios, and *FT* levels are the major determinants of plant shade-induced flowering timing[29, 30, 50], and because the R/FR=1 condition is enough to induce *FT* in the morning, we investigated the more comprehensive relationship between R/FR ratios and *FT* levels. Also, we analyzed whether the *phyA* and *elf3* mutations affect *FT* levels in LD with different R/FR ratios. In WT plants, there is nearly a linear relationship between the decrease in the R/FR ratios and the increase in *FT* mRNA levels in the morning (ZT4) and the afternoon (ZT16) (Fig. 4g, h). In the *phyA-211* mutant, morning *FT* induction was severely reduced under a wide range of R/FR ratios, while morning *FT* levels in the *elf3-1* mutant were constantly high (Fig. 4g). In both *phyA-211* and *elf3-1* mutants, *FT* levels over different R/FR ratios stayed at nearly similar levels at ZT4 (Fig. 4g), indicating that the function of both proteins is required to tune *FT* levels in response to R/FR ratio changes during the morning. In the afternoon, the lack of *elf3* made the plants more sensitive to the R/FR ratio changes with a large increase in *FT* expression under lower R/FR ratios (Fig. 4h). There was only a small *phyA-211* mutation effect on

afternoon *FT* expression levels (Fig. 4h). Taken together, these results suggest that both phyA and ELF3 likely have time-dependent functions in light quality-controlled *FT* level regulation.

We next studied the genetic relationship between *PHYA* and *ELF3* in the regulation of *FT*. There was an intermediate level of *FT* expression in the *phyA-211 elf3-1* double mutant compared to the *FT* level in each mutant examined under all conditions (Supplementary Fig. 19), indicating that phyA and ELF3 function antagonistically on *FT* regulation. As a biochemical study indicated the presence of a phyA-ELF3 complex[49], we examined whether our modified LD conditions influence the amount of phyA co-immunoprecipitated with ELF3 protein. In LD, phyA protein dissociated from the ELF3 complex as soon as the light was turned on, while in both LD+FR and LD+FR+temp conditions, similar amounts of phyA were co-immunoprecipitaed with ELF3 at later time points during the morning (Supplementary Fig. 20). These results suggest that the prolonged presence of the phyA-ELF3 complex in LD+FR+temp may change the expression levels and/or activity of phyA and/or ELF3 proteins.

We also analyzed the phyA and ELF3 protein expression patterns in LD+FR+temp to investigate potential changes. The accumulation levels of phyA protein in LD+FR+temp were higher during the morning than in LD, although it eventually degraded by the end of the day (Fig. 4i). This is likely controlled by posttranslational regulation, since *PHYA* transcript levels under these conditions were very similar (Supplementary Fig. 21a). In contrast, the ELF3 protein levels in LD+FR+temp were lower throughout the day than in LD (Fig. 4j). The *ELF3* transcript levels in LD+FR+temp were also slightly lower than in LD (Supplementary Fig. 21b). These results indicate that ELF3 protein level changes may be transcriptionally and posttranslationally regulated. Higher expression of *FT* at ZT4 in

LD+FR+temp is consistent with the higher level of its activator phyA and lower levels of its repressor ELF3 under these conditions.

We further analyzed whether ELF3 affects phyA protein patterns or *vice versa*. In LD+FR+temp, there was no difference in *PHYA* transcript levels between WT and the *elf3* mutant (Supplementary Fig. 22a). The phyA protein levels were slightly higher in the *elf3* mutant than in the WT plants, although the difference was not statistically significant (Supplementary Fig. 22c). There was less ELF3 protein in the *phyA* background than in WT without affecting transcript levels (Supplementary Fig. 22b, d), suggesting that phyA may regulate ELF3 protein levels posttranscriptionally in LD+FR+temp. However, since ELF3 is a repressor of *FT*, the reduction of ELF3 levels in the *phyA* mutants cannot be the major cause of the reduction of *FT* levels in *phyA*. Previous work showed that ELF3 forms a complex with a large number of light signaling and circadian clock components, many of which require functional phyB to physically associate with the ELF3 complex[49]. In addition, more phyA protein was co-immunoprecipitated with ELF3 after dawn under LD+FR+temp conditions (Supplementary Fig. 20). These results let us hypothesize that phyA may affect ELF3 function by directly modulating the interaction of ELF3 with other factors in a light/temperature-dependent manner.

We therefore tested whether phyA directly influences the composition of the ELF3 complex, which may affect *FT* levels. To assess this possibility, we harvested *ELF3:ELF3-6H3F* samples with/without the *phyA* mutation in the morning of LD+FR+temp conditions, and identified peptides co-immunoprecipitated with ELF3 using mass spectrometry analysis. We included *ELF3:ELF3-6H3F/phyB* as a reference. When we compared our peptide list of *ELF3:ELF3-6H3F* samples with previous ones harvested in the afternoon[49], we noticed that our list did not contain peptides from ELF3-associated circadian clock proteins (Supplementary Table 2), suggesting that ELF3 does not assemble with the same Evening

373 Complex in the morning. We identified peptides derived from COP1 but not SPA1. phyB is
374 still important for ELF3 complex formation in the morning. The loss of *phyA* did not seem to
375 drastically change the composition of the ELF3 complex, although fewer peptides from
376 COP1 and phyE were detected in the *phyA* background (Supplementary Table 2). These
377 results indicate that phyA may affect the interaction of a small number of components in the
378 ELF3 complex. However, these results are not sufficient to evaluate whether those changes
379 may affect either ELF3 function or *FT* transcription in the *phyA* mutant under LD+FR+temp
380 conditions. Further analysis is required to elucidate the exact mechanism by which phyA and
381 ELF3 antagonistically regulate *FT* levels in LD+FR+temp.

382 As *CO* is required for the *FT* morning peak (Fig. 4a), and the *cop1* and *spa* triple
383 mutants showed increased *FT* levels in LD+FR+temp (Supplementary Fig. 16c, d), we
384 hypothesized that CO protein levels may increase under these conditions. To test this, we
385 analyzed the diurnal expression profile of CO protein in *CO:HA-CO* plants[51] in LD and
386 LD+FR+temp. The overall accumulation patterns of CO protein in LD and LD+FR+temp
387 were similar (Fig. 5a). However, we noticed that CO protein increased more in LD+FR+temp
388 than in LD at the ZT4 time point, when the *FT* morning peak was induced (Fig. 5a).
389 Therefore, we analyzed a fine scale time course of CO protein profiles under the same
390 conditions during the morning. In LD, CO protein acutely accumulated just after dawn
391 (ZT0.5-1) but quickly degraded by ZT2 (Fig. 5b). In LD+FR+temp, CO protein levels kept
392 increasing until ZT1, and then decreased more gradually during the morning. The levels of
393 CO protein expressed in the morning of LD+FR+temp was similar to or potentially higher
394 than the levels around dusk (Fig. 5a, b), suggesting that the elevation of CO protein levels in
395 LD+FR+temp might contribute to morning *FT* peak generation.

396 CO protein levels are controlled by several E3 ubiquitin ligases, such as the
397 COP1/SPA complex[44, 45]. Both phyA and ELF3 physically interact with the COP1/SPA1

complex to regulate its function[49, 52, 53]. We therefore investigated whether phyA and/or ELF3 mediate *FT* regulation through regulation of CO protein stability. We found that ELF3 is in the same CO protein complex *in planta* and *in vivo* (Fig. 5c and Supplementary Fig. 23). In addition, *FT* expression and the early flowering phenotype of *elf3-1* were largely dependent on functional *CO,* as *FT* expression levels are very low in both *co-101* and *elf3-1 co-101*, and *elf3-1 co-101* flowered just slightly earlier than the late flowering *co-101* mutant (Supplementary Fig. 24). Although the results of the *FT* levels in the *elf3-1 co-101* double mutant are similar to those in the previously characterized *elf3-1 co-1* double mutant[54], the *elf3-1 co-1* double mutant showed an intermediate flowering phenotype between the *co-1* and *elf3-1* mutants[54]. This flowering time difference might be caused by the difference in the genetic backgrounds (*elf3-1 co-1* in F3 segregants between Col-0 and Landsberg[55] cross, vs. *elf3-1 co-101* in Col-0) and/or *co* alleles. We next analyzed whether ELF3 influences CO stability, and found that CO protein was more abundant in the *elf3* mutant, including at ZT4 (Fig. 5d and Supplementary Fig. 25). Together with our results that showed lower levels of ELF3 protein in LD+FR+temp, these results indicate that ELF3 may negatively influence CO stability in the morning, and that LD+FR+temp conditions in part reduce the amount of the negative regulator to increase CO protein stability, consistent with increased expression of its target *FT*.

Discussion

Our results indicate that the difference in R/FR ratios (either 1 or 2) and daily temperature are the main causes of the difference in flowering time between natural LD and lab LD conditions. Mechanistically, this difference in growth conditions likely causes different expression levels of the florigen genes, *FT* and *TSF,* especially in the morning. Previous work indicated that *FT* transiently expressed between ZT12 and ZT20 in SD was more effective for floral induction than *FT* induced during other time windows[25]. How does

morning-expressed *FT* affect flowering compared to evening-expressed? The uploading of FT proteins into the phloem and the unloading of them into the shoot apical meristem seems to be actively regulated, at least in cucurbit plants[56, 57]. Phloem flux and the concentration of major transport sugars in phloem sap exhibit diurnal and developmental changes in some plants[58, 59, 60]. Therefore, the efficiency of florigen movement may change depending on growth conditions, time of day, and plant age. Although it is beyond the scope of our current research, it would be of interest to assess whether the timing of *FT* expression during the morning has some mechanical advantages compared to evening in natural LD.

Our results obtained from plants grown in LD+FR+temp conditions indicate that phyA and ELF3 are likely involved in the regulation of the morning expression of *FT* in natural LD (Fig. 5e, f). In addition, CO protein, a master activator of *FT*, is likely more stable in the morning of natural LD than in regular lab LD. This may partly contribute to higher induction of *FT* in the morning. However, as CO protein is known to interact with several other transcription factors to regulate *FT* in the morning[61], it would be too simple to speculate that this increase in CO protein stability is a major cause of morning *FT* induction. We assume that there are still other known and unknown factors that participate in controlling *FT* expression levels during the morning in natural LD (Fig. 5e, f). We therefore think the findings presented in this manuscript are a starting point to understanding the mechanisms of the previously uncharacterized florigen induction that takes place in natural LD.

With the external coincidence model for explaining photoperiodic response as a basis[62], molecular mechanisms that consist of complex interplay between light signaling and the circadian clock have been proposed to explain LD specific dusk expression of *FT* [1]. Although our results indicate the involvement of some known photoperiodic flowering regulators in morning *FT* induction, the current proposed mechanism cannot explain how

447 these factors specifically induce *FT* in the morning in natural LD. Investigating these
448 mechanisms will help us to understand how *Arabidopsis* plants flower in spring in nature.
449 Behavioral rhythms in model animals (*Drosophila*, mouse, and golden hamster)
450 differed between natural and lab conditions[63, 64, 65]. At least in *Drosophila*, transcriptional
451 levels of clock genes were altered between these two conditions[66]. Even for *Arabidopsis*,
452 previous work also reported discrepancies in predicted flowering phenotypes when
453 *Arabidopsis* flowering mutants were grown outside, although the molecular mechanism that
454 caused this was unknown[16]. Based on our current work, the discrepancies might be partly
455 caused by the difference in light quality and temperature between lab and natural conditions.
456 To understand plant response at molecular levels in nature, recent functional genomic
457 approaches in molecular ecology have successfully revealed certain mechanisms by which
458 plants sense specific environmental stimuli in complex natural environments[67, 68]. However,
459 these approaches still have geographical and environmental limitations. Our approach for
460 optimizing simplified lab conditions based on plant response in nature will be widely feasible
461 for anyone who studies plant physiology and development in the lab. Studying plant
462 responses under refined lab conditions that more closely reflect natural conditions will likely
463 fill the current gap between genetics and ecology and facilitate interdisciplinary
464 communication between them in order to more holistically understand the underlying
465 mechanisms of ever-changing phenological response in plants.
466
467 **Figure legends:**
468 **Fig. 1: The florigen *FT* gene is induced in the morning in natural LD. a**, Changes in light
469 intensity and temperature on the days near the summer solstice in 2013 when the samples
470 were harvested. For outside conditions, Zeitgeber time 0 (ZT0) was set as the sunrise time
471 (i.e. 5 AM in Seattle from 6/23/13 to 6/25/13). Light intensity results are means ± SEM from

different growth areas (n=3). Temperature data were obtained from a nearby weather station. **b**, **c**, Expression profiles of *CO* (**b**) and *FT* (**c**) under the conditions shown in (**a**). All gene expression results (means ± SEM) in this manuscript were normalized against *IPP2* and *PP2A* (n=3). **d**, Flowering time results of plants grown outside in June and in lab LD. Each box is located between the upper and the lower quartiles. The thick horizontal lines in the boxes represent the median, and open diamonds represent the mean. Outliers are indicated by circles. ($12 \leq n \leq 100$, *** $p<0.001$, ns: non-significant). **e**, *FT* expression profiles in wild-type (WT: Col-0) plants, *fkf1*, and *gi-2* mutants grown outside around the summer solstice. **f**, *FT* expression profiles in WT grown at different times in spring. **g**, *FT* expression profiles in WT grown around the summer solstice in Seattle and Zürich. **h**, Flowering phenotypes of WT plants grown in different months and locations in spring. The details of the box plots are the same as those in Fig. 1d ($n \geq 11$, ** $p<0.01$, *** $p<0.001$, ns: non-significant).

Fig. 2: Adjusting the R/FR ratio to 1 and changing the daily temperature of the lab growth conditions are sufficient to recreate the *FT* profiles and flowering of plants grown in natural LD. **a**, *FT* expression profiles in LD and LD+FR. **b**, *FT* expression profiles in LD, LD+FR+temp, and outside in 2014. **c**, Flowering phenotypes of WT accessions and photoperiodic mutants in LD+FR+temp. Each box is located between the upper and the lower quartiles. The thick horizontal lines in the boxes represent the median, and open diamonds represent the mean. Outliers are indicated by circles. ($n \geq 11$, * $p<0.05$, ** $p<0.01$, *** $p<0.001$, ns: non-significant). **d**, Spatial expression patterns of *FT* in LD+FR+temp. *FT:GUS* plants were grown in LD+FR+temp for two weeks and harvested at ZT4. As a comparison, the *FT:GUS* plants were grown in LD and harvested at ZT4. The staining patterns of GUS activity in the LD-grown samples harvested in ZT4 resembled those

496 in the ones harvested at the end of the day (ZT16) (Supplementary Fig. 13), most likely due
497 to the very stable nature of the GUS protein[69]. Scale bar=1 mm.
498
499 **Fig. 3: Morning induction of florigen expression occurs under both natural LD and**
500 **LD+FR+temp conditions, and is a common response in wild-type accessions.**
501 **a**, The upregulated genes of RNA-seq results in two-week-old samples harvested at ZT4 in
502 2013, 2014, and LD+FR+temp conditions compared with the ZT4 samples in LD. The GO
503 term categories enriched in the 57 genes are shown. Supplementary Table 1 shows actual
504 values of fold changes. **b**, Flowering-related genes in FLOR-ID were extracted from the
505 dataset shown in (E). **c**, *FT* expression levels in the morning (ZT4) and at dusk (ZT16) in 20
506 *Arabidopsis* WT accessions (Supplementary Fig. 15) in LD and LD+FR+temp.
507
508 **Fig. 4: phyA and ELF3 are involved in the regulation of morning *FT* expression in**
509 **LD+FR+temp. a**-**c**, *FT* expression profiles in WT plants, *co-101*, and *phyA-211* mutants in
510 LD+FR+temp (**a**), LD (**b**), and LD+FR (**c**). **d**-**f**, *FT* expression profiles in WT plants, *phyB-9*,
511 and *elf3-1* mutants in LD+FR+temp (**d**), LD (**e**), and LD+FR (**f**). **g**, **h**, *FT* levels in WT
512 plants, *phyA-211*, and *elf3-1* mutants in LD with different R/FR ratios. The levels of *FT* in
513 these plants in the morning, ZT4 (**g**), and at dusk, ZT16 (**h**). **i**, Daily accumulation patterns of
514 phyA protein in LD and LD+FR+temp. **j**, Daily accumulation patterns of ELF3 protein in
515 *ELF3:ELF3-6H3F* plants in LD and LD+FR+temp. For both (**i**) and (**j**), the representative
516 blot images are shown. Actin was used as a loading control. The protein quantification results
517 are means ± SEM derived from six biological replicates in this manuscript.
518
519 **Fig. 5: CO protein stability was increased in LD+FR+temp during the morning. a**, **b**,
520 CO protein accumulation patterns in *CO:HA-CO* plants in LD and LD+FR+temp. Histone H3

was used as a loading control. **c**, Coimmunoprecipitation analysis of ELF3 and CO proteins. *35S:ELF3-6H3F*, *35S:3HA-CO*, and *35S:3HA-CO/35S:ELF3-6H3F* plants were grown in LD, LD+FR (labeled as FR), or LD+FR+temp (FR+temp) and harvested in the morning (ZT4). The experiments were repeated, and similar results were obtained. **d**, CO protein accumulation patterns in *CO:HA-CO* and *CO:HA-CO*/*elf3-1* plants grown in LD+FR+temp. **e**, **f**, A model for CO-dependent *FT* regulation under natural LD conditions. This model shows temporal expression patterns of CO protein (top) and *FT* transcripts (bottom) under lab LD (**e**) and natural LD (**f**) conditions. **e**, Under artificial lab LD conditions in which the R/FR ratio is equal to or greater than 2 and the temperature is constant, CO protein appears to immediately accumulate after light onset and then rapidly degrade, resulting in low levels of CO protein in the morning and early afternoon. During this period, ELF3 protein inhibits *FT* expression through an unknown mechanism. CO protein peaks again at the end of the day, which directly activates *FT* transcription under these conditions. **f**, Under natural LD conditions, the R/FR ratio is 1 and the ambient temperature oscillates throughout the day. The amount of phyA protein increases in the morning, whereas the amount of ELF3 protein decreases (Fig. 3i, j). CO protein accumulates rapidly at high levels after sunrise, and CO protein degrades more slowly under natural LD conditions than under lab LD conditions. This CO accumulation might be important for morning induction of *FT*. In addition to the CO protein stability changes, there might be other factors (depicted as "X") involved in the induction of morning *FT* under natural LD conditions. The phyA signal is positively involved in *FT* induction under these conditions. ELF3 negatively acts on *FT* regulation under these conditions. In addition, the temperature oscillations strongly repress *FT* transcription in the evening. Therefore, although CO protein abundance is high even at dusk, the levels of *FT* expression remain relatively low around dusk compared to morning. We showed that we can

recreate these *FT* expression profiles in the lab by simply adjusting the R/FR ratio of light source and temperature conditions.

Acknowledgments: We thank Drs. Motomu Endo, Mathias Zeidler, Xing Wang Deng, Ute Hoecker, Rachel Green, Stacey Harmer, Takafumi Yamashino, and Ji Hoon Ahn for providing the mutant seeds, Dr. Jennifer Nemhauser for critical reading of the manuscript, and Jeanette Milne for technical support. This work was supported by NIH grant (GM079712) to T.I., NSF grants (IOS-1656076 to TI, and IOS-1456796 to D.A.N.), Next-Generation BioGreen 21 Program (SSAC, PJ013386, Rural Development Administration, Republic of Korea) to Y.H.S. and T.I., JST CREST Grant (JPMJCR16O3) and Swiss National Science Foundation to K.K.S., and NRF grant (NRF-2015R1D1A1A01058948) to Y.H.S. We acknowledge NSF grant (DBI-0922879) for LTQ-Velos Pro Orbitrap LC-MS/MS acquisition. A.K. is supported by the JSPS Postdoctoral Fellowships for Research Abroad.

Author contributions: T.I. conceived the project, and Y.H.S., A.K., and T.I. designed the experiments. Y.H.S., A.K., M.S.K., M.F.C., N.L., E.R.T., D.L.C., D.Y.H., R.A., S.K.H, H.H., N.H.N, D.A.N., A.J.M., and T.I. performed experiments and analyses, Y.H.S., A.K., and T.I. wrote the manuscript with the help of R.A., D.A.N., A.J.M., and K.K.S.

Competing interests: Authors declare no competing interests.

Materials and Correspondence: Correspondence and requests for materials should be address to T.I (takato@uw.edu) and Y.H.S. (younghsong@ajou.ac.kr).

Methods:

Plant materials and growth conditions.

Except where indicated, all *Arabidopsis thaliana* plants, wild type (WT), *fkf1*[70], *fkf1-2*[21], *gi-2*[26], *ft-1* and *ft-1 tsf-1*[71], *ft-101* and *co-101*[72], *phyA-211*[35], *phyB-9*[73], *elf3-1* [74], *fhy1-3 fhl-1*[75], *cop1-6*[76], *spa1-3 spa3-1 spa4-1*[77], *pif1 pif3 pif4 pif5* (*pifq*)[78], *cry1* (*hy4-2.23N*) *cry2-1*[79], *cca1-1* lhy-Null*[80], *prr7-11 prr9-10*[81], *hos1-3*[48], *svp-32*[82], *svp-32 flm-3 flc-3*[33], *ELF3:ELF3-6H3F*[49], *CO:HA-CO* and *35S:3HA-CO*[51], and *FT:GUS* [72], used in this study are in the Columbia-0 (Col-0) background. *phyA-201* is in the Landsberg *erecta* (L*er*) background[35]. The *ft-1* and *ft-1 tsf-1* seeds were kindly provided by Dr. Motomu Endo. The *fhy1-3 fhl-1* seeds were kindly provided by Dr. Mathias Zeidler. The *cop1-6* seeds were kindly provided by Dr. Xing Wang Deng. The *spa1-3 spa3-1 spa4-1* seeds were kindly provided by Dr. Ute Hoecker. The *cca1-1* lhy-Null* seeds were kindly provided by Drs. Rachel Green and Stacy Harmer. The *prr7-11 prr9-10* seeds were kindly provided by Dr. Takafumi Yamashino. The *svp-32* and *svp-32 flm-3 flc-3* seeds were kindly provided by Dr. Ji Hoon Ahn. Wild-type *Arabidopsis* accessions, Oy-1, RLD-1, Mh-0, An-1, Nos-0, Ma-1, Rd-0, Nd-1, En-1, Jl-3, Kz-9, Di-G, Wei-0, Ka-0, Sei-0, Mt-0, and Van-0 were all obtained from the ABRC stock center at Ohio State University. The *phyA-211 elf3-1* double mutant was generated by a genetic cross between *phyA-211* and *elf3-1*. The *co-101 elf3-1* double mutant was generated by a genetic cross between *co-101* and *elf3-1*.

To generate *35S:ELF3-6H3F* transgenic lines, the pENTR/D-TOPO vector harboring the full length of *ELF3* cDNA without a stop codon[49] was transferred to pB7HFC binary vector[49]. The *35S:ELF3-6H3F* construct in pB7HFC was transformed into *elf3-1* plants. For *ELF3:ELF3-6H3F/phyA-211* lines, the *ELF3:ELF3-6H3F* construct in pK7HFC vector[49] was introduced to *phyA-211* plants. To generate *35S:3HA-CO/35S:ELF3-6H3F* lines, the *35S:3HA-CO* construct in pH7WG2 (ref 51) was transformed into the *35S:ELF3-6H3F* line. The transgenic plants were selected based on the expression levels of both *CO* and *ELF3*

595 genes. For *CO:HA-CO/elf3-1* lines, the *CO:HA-CO* construct in pPZP221 binary vector[51]
596 was transformed into *elf3-1* plants.

597 All plants were grown either on soil in standard flats with inserts (STF-1020-OPEN
598 and STI-0804, T.O. Plastics; for plants grown in Seattle or similar flats/inserts for plants
599 grown in Zürich and Edinburgh) or in sterile 1X Linsmaier and Skoog (LS) agar media
600 (Caisson) without sucrose. The soil (Sunshine Mix #4, Sun Gro Horticulture) contained a
601 slow release fertilizer (Osmocote 14-14-14, Scotts Miracle-Gro) and a pesticide (Systemic
602 Granules, Bonide). After seeds were sown onto soil or growth media, they were stratified in a
603 4°C room for at least three days and then transferred to outside growth areas or growth
604 chambers. Only non-transgenic plants were used for the outdoor experiments, following
605 institutional, national, and international restrictions on handing genetically modified
606 organisms (transgenic plants were only used in certified lab settings). For outside
607 experiments, the flats containing stratified seeds were transferred onto a platform in a low
608 tunnel equipped with a shading filter in our caged plant growth areas (University of
609 Washington, University of Zürich, and University of Edinburgh). To avoid shading effects
610 from neighboring plants, seeds were sown at a low density, and when necessary, younger
611 seedlings were thinned to let individuals grow separately. To prevent potential light stress
612 from excess direct sunlight exposure (which can be stronger than 1000 $\mu mol/m^2/s$), the cage
613 was covered with double layers of Reemay Garden Blanket (Reemay) to reduce sunlight
614 intensity without changing the red/far-red ratio (R/FR). The R/FR ratio was measured by
615 LightScout Red/Far Red meter (Spectrum Technologies), as well as UV-VIS Spectrometer
616 (StellarNet Inc). The light intensity changes around the summer solstice were measured using
617 LI-250A light meter (LI-COR). Temperature was directly monitored by HOBO Pendant
618 Temperature/Light 64K Data Loggers (Onset) for Edinburgh as well as Seattle. Air
619 temperature was obtained from nearby weather station data,

https://www.ed.ac.uk/geosciences/weather-station/weather-station-data for Edinburgh, http://www.meteoswiss.admin.ch/home/research-and-cooperation/nccs.html for Zurich, and http://www-k12.atmos.washington.edu/k12/grayskies/nw_weather.html for Seattle, as shown in Supplementary Fig. 1. Information regarding sunrise time (ZT0) and day length in Seattle was obtained from http://aa.usno.navy.mil/data/docs/RS_OneYear.php.

Normal lab LD and SD conditions were described previously[51]. For FR light supplement in LD+FR and LD+FR+temp conditions, weak 730 nm far-red LED light (RAY "PfrSpec", Fluence Bioengineering, previously referred to as BML Horticulture) was provided together with full-spectrum white fluorescent light (F017/950/24", Octron Osram Sylvania) in order to set the R/FR=1. To obtain dim far-red light, we used a dimmer (Fluence Bioengineering/BML Horticulture) with the LED light source and also wrapped the LED light with a single layer of regular white copy paper. The R/FR ratio was adjusted using LightScout Red/Far Red meter (Spectrum Technologies), and confirmed using UV-VIS spectrometer.

To apply LD+light intensity conditions, light intensity changes during the daytime shown in Supplementary Fig. 8a were set based on averages of three day-long light intensity measurements shown in Fig. 1a. Specific settings in growth chambers were as follows: ZT0, 0 $\mu mol/m^2/s$; ZT1, 29 $\mu mol/m^2/s$; ZT4, 84 $\mu mol/m^2/s$; ZT7, 173 $\mu mol/m^2/s$; ZT10 148 $\mu mol/m^2/s$; ZT13, 81 $\mu mol/m^2/s$; and ZT16, 0 $\mu mol/m^2/s$. The light intensity between two settings was gradually changed in a ramping mode. The light intensity changes in the chamber were confirmed using LI-250A light sensor (LI-COR).

For temperature fluctuation settings in LD+temp and LD+FR+temp conditions, temperature data for seven days around the summer solstice of 2013, from June 21st to 27th , in Seattle was obtained from a website (http://www-k12.atmos.washington.edu/k12/grayskies/nw_weather.html) and averaged. Based on the

average temperature data, a multi-step program shown in Supplementary Fig. 8g was set in ramping mode as follows: ZT0, 15.9°C; ZT2, 16.2°C; ZT4, 17.9°C; ZT5.8, 19.4°C; ZT9, 22.2°C; ZT10.4, 22.6°C; ZT11, 22.8°C; ZT12, 22.1°C; ZT16, 19.8°C; ZT17, 18.3°C; ZT20, 16.6°C; ZT23, 15.8°C. The temperature changes were confirmed using HOBO Pendant Temperature/Light 64K Data Loggers (Onset).

Flowering time was measured by the number of rosette and cauline leaves on the main stem when inflorescence reached 1-5 cm high as described previously[51]. Flowering time experiments were performed with 12 individual plants at a minimum. All flowering time results in this manuscript are means ± standard errors of means (SEM).

RNA preparation and gene expression analyses.

For gene expression analyses, 14-day-old seedlings grown on soil (all outside grown samples) or LS agar plates (samples grown in the incubators) were harvested every 3 hours during a 24-h period and were used for RNA extraction. RNA extraction, cDNA synthesis, Q-PCR conditions and normalization by *IPP2+PP2A* were described previously[83]. Primers and PCR conditions for *CCA1*, *LHY*, *PRR9*, *PRR7*, *PRR5*, *TOC1*, *CDF1*, *FKF1*, *GI*, *CO*, *FT*, *FLC*, *SVP*, *ISOPENTENYL PYROPHOSPHATE/DIMETHYLALLYL PYROPHOSPHATE ISOMERASE* (*IPP2*), and *SERINE/THREONINE PROTEIN PHOSPHATASE 2A* (*PP2A*) were previously described[22, 23, 83, 84]. All expression results were normalized using averages of *IPP2* and *PP2A* values. The remaining primer sequences used for analyzing gene expression profiles are the following: 5'-GCACAGACTGATTAAGGTTCAAAAAC-3' and 5'-CTTCACTGGATAGCTTTTAGCAG-3' for *ELF3*; 5'-AATCTAGAGATCAGGTTAACGC-3' and 5'-CTTCTTCTGACACATCTTCCT-3' for *PHYA*; 5'-CTCGGGAATTCATCGTATTG-3' and 5'-CCTCTGGCAGTTGAAGTAAG-3' for *TSF*. Q-PCR for *CCA1*, *LHY*, *PRR9*, *PRR7*, *PRR5*, *TOC1*, *CDF1*, *GI*, *SVP*, and *IPP2* was

done using the following program: 1 min at 95°C, followed by 40-50 cycles of 10 sec at 95°C and 20 sec at 60°C. Q-PCR for *FKF1*, *CO*, *FT*, *TSF*, *ELF3*, *PHYA*, and *PP2A* was done using the following program: 1 min at 95°C, followed by 40-50 cycles of 10 sec at 95°C, 15 sec at annealing temperature, and 15 sec at 72°C. Annealing temperature for each primer set was 55°C for *FKF1* and *CO*, 64°C for *FT*, 59°C for *TSF*, 61°C for *ELF3*, 64.3°C for *PHYA*, and 64°C for *PP2A.*

Whole transcriptome RNA-sequencing (RNA-seq) analysis.

Wild-type plants were grown on soil under LD, LD+FR+temp and natural LD conditions and harvested at ZT4 on day 14. The "2013 outside" samples were harvested on 6/25/13, and the "2014 outside" samples were harvested on 7/7/14. After mRNA was purified using NEB Next Poly(A) mRNA magnetic isolation kit (New England Biolabs), RNA-seq libraries were prepared using the YourSeq 3'-Digital Gene Expression RNAseq Library Kit (Amaryllis Nucleics). A Bioanalyzer 2100 (Agilent, High Sensitivity DNA Kit) was used for library quality control, to determine average library size, and together with concentration data from a Qubit 2.0 Fluorometer (Life Technologies, dsDNA High Sensitivity Assay Kit) to determine individual library molarity and pooled library molarity. Pooled libraries were sequenced on a NextSeq 500 (Illumina, High Output v2 75 cycle kit) to yield single-read 80 bp reads.

FASTQ sequence files were preprocessed in two steps. A Python library (clipper.py, https://github.com/mfcovington/clipper) was used to trim off the first 8 nucleotides of each read to remove potential mismatches to the reference sequence caused by annealing of a random hexamer required for library synthesis. Trimmomatic v0.36[85]; http://www.usadellab.org/cms/?page=trimmomatic] was used to remove adapter sequences and trim or filter reads based on quality. The parameters used for Trimmomatic were

"ILLUMINACLIP:TruSeq3-PE-2.fa:2:30:10 LEADING:3 TRAILING:3 SLIDINGWINDOW:4:15 MINLEN:50".

Preprocessed reads were mapped to the *Arabidopsis thaliana* TAIR10 cDNA reference sequence (ftp://ftp.ensemblgenomes.org/pub/plants/release-34/fasta/arabidopsis_thaliana/cdna/Arabidopsis_thaliana.TAIR10.cdna.all.fa.gz) using bowtie2 with the "--norc" parameter to enforce strand-specific alignment. Read counts for each transcript in the cDNA reference were calculated using a Perl script (simple_counts.pl, https://github.com/mfcovington/read_counter).

The R package edgeR[86] was used to identify differentially expressed transcripts between samples grown in lab LD conditions and samples grown in LD+FR+temp conditions, outdoor samples from 2013 and 2014. Transcripts were retained for analysis if they had more than two counts per million in at least three samples. After normalization factors were calculated and dispersion estimated, pairwise comparisons were performed using edgeR's exact test. Differentially expressed genes were then filtered using a false discovery rate (FDR) cutoff of 0.05 and a minimum log2 fold change of 1. FDRs were calculated by adjusting P-values for multiple comparisons using the Benjamini–Hochberg procedure[87].

Differential gene expression results were annotated using TAIR10 gene and transcript descriptions (https://www.arabidopsis.org/download_files/Genes/TAIR10_genome_release/gene_description_20131231.txt.gz). Gene ontology analysis was performed using DAVID[88].

GUS staining.

For histochemical staining of GUS activity for tissue-specific expression of the *FT* gene, 14-day-old *FT:GUS* plants grown under LD, LD+FR and LD+FR+temp conditions were harvested either at ZT4 (LD+FR and LD+FR+temp grown samples) or at both ZT4 and ZT16

(LD grown samples), and immediately treated with 90% pre-chilled acetone on ice for 10-15 min to fix and extract chlorophylls. After washing three times with 100 mM Na-phosphate pH7.0, whole plant tissues were submerged in the staining solution (100 mM Na-phosphate pH7.0, 10 mM EDTA, 0.5 mM Potassium ferricyanide, 0.5 mM Potassium ferrocyanide, 0.1% Triton X-100, and 1 mM X-Gluc). After 4-hour staining, the tissues were washed and dehydrated with ethanol series 30%, 50%, 80%, and 100%.

Tandem affinity purification coupled mass spectrometry (TAP-MS) analysis.

Fourteen-day-old *ELF3:ELF3-6H3F* and *ELF3:ELF3-6H3F/phyA-211* lines grown on LS agar plates under the LD+FR+temp conditions were harvested at ZT4. Procedures for Tandem FLAG and His-immunoprecipitations (IP), protein digestion, and liquid chromatography-tandem mass spectrometry (LC-MS/MS) were performed according to Huang *et al.*[49].

Statistical analysis.

Statistical analyses for flowering time experiments were done using R Statistical Computing software (v3.2.3; R Core Team, 2015). The effect of conditions on flowering time was tested using linear models (lm) when the assumptions were met in 'gvlma' function in the 'gvlma' package. When the assumptions were not met, generalized linear models (glm) with poisson error distribution (faily=poisson) were used. For more than two groups, pairwise comparisons were conducted with Tukey's multiple comparisons adjustment using 'glht' function in the 'multcomp' package.

Immunoblot analysis and protein quantification.

744 For analyzing diurnal expression profiles of phyA, ELF3, and CO proteins, 14-day-
745 old *Arabidopsis* seedlings grown on LS agar media under LD or LD+FR+temp conditions
746 were harvested at each time point, frozen in liquid nitrogen, and stored at -80 ºC. Total
747 proteins were extracted using extraction buffer [50 mM Na-phosphate pH7.4, 100 mM NaCl,
748 10% glycerol, 5 mM EDTA, 1 mM DTT, 1% NP-40, 0.5% SDS, 0.5% Sodium deoxycholate,
749 50 μM MG-132, 2 mM $NaVO_4$, 2 mM NaF, and protease inhibitor tablets-EDTA free
750 (Pierce)], and nuclei samples were prepared using CelLytic Plant Nuclei Isolation/Extraction
751 Kit (Sigma) based on manufacturer protocol.
752 To detect proteins, total protein extract for phyA and ELF3, or nuclear extract for CO,
753 were resolved in 9% or 11-12% SDS-PAGE gels, respectively, and transferred to
754 nitrocellulose membranes (Bio-rad). phyA, ELF3-6H3F, and HA-CO proteins were detected
755 using a monoclonal anti-phyA antibody[89] kindly provided by Dr. Akira Nagatani, anti-FLAG
756 (A8592, Sigma), and anti-HA (3F10, Roche) antibodies. Actin or Histone H3 proteins were
757 used for internal loading controls of total protein or nuclear extract, respectively, and detected
758 by anti-actin (C4, Millipore) and anti-histone H3 (ab1791, Abcam) antibodies, respectively.
759 For protein quantification, immunoreactive proteins on immunoblotted membranes were
760 visualized with SuperSignal West Pico Luminol/Enhanced Solution (Thermo) and/or ECL
761 Select Western Blotting Detection Reagent (Amersham) and imaged by ChemiDoc Touch
762 (Bio-rad). The image was used for quantification with the Image Lab program (Bio-rad).
763 Relative protein abundance was normalized against Actin or Histone H3.
764
765 **Co-immunoprecipitation experiments.**
766 To analyze *in vivo* interactions, the *ELF3:ELF3-6H3F*, *35S:ELF3-6H3F*[49], *35S:3HA-*
767 *CO*, and *35S:3HA-CO 35S:ELF3-6H3F* lines grown under LD, LD+FR, or LD+FR+temp
768 conditions were harvested at ZT0, ZT2, or ZT4 on day 14, frozen in liquid nitrogen, and

stored at -80 ºC. For analyzing *in planta* interactions, the *35S:ELF3-6H3F*, *35S:3HA-CO*[51], and *35S:CO-TAP*[51] constructs were infiltrated into 3-week-old *Nicotiana benthamiana* leaves as described[51].

The method for coimmunoprecipitation (Co-IP) assays was described previously[51]. Briefly, proteins were extracted from 1 ml volume of ground tissues using Co-IP buffer [50 mM Na-phosphate pH7.4, 150 mM NaCl, 10% glycerol, 5 mM EDTA, 1 mM DTT, 0.1% Triton X-100, 50 μM MG-132, 2 mM $NaVO_4$, 2 mM NaF, and protease inhibitor tablets-EDTA free (Pierce)] and incubated with Protein G-coupled magnetic beads (Dynabeads Protein G, Invitrogen) that captured anti-FLAG (F1804, Sigma) antibody at 4 ºC for 10 minutes under dim light. After washing three times, precipitated proteins were eluted with 2X SDS sample buffer at 80 ºC for three minutes. Fifty percent of the eluted proteins and 1.5% of the total extract as an input were resolved in 9% SDS-PAGE gels. ELF-6H3F and endogenous phyA proteins were detected by western blot using anti-FLAG (Sigma) and anti-phyA antibodies, respectively.

Data availability.

All data is available in the main text or the supplementary materials. The raw sequence data (GSE110605) were deposited in NCBI Sequence Read Archive.

References:

1. Song YH, Shim JS, Kinmonth-Schultz HA, Imaizumi T. Photoperiodic flowering: time measurement mechanisms in leaves. *Annu Rev Plant Biol* **66**, 441-464 (2015).
2. Wood S, Loudon A. Clocks for all seasons: unwinding the roles and mechanisms of circadian and interval timers in the hypothalamus and pituitary. *J Endocrinol* **222**, R39-59 (2014).

794 3. Mouradov A, Cremer F, Coupland G. Control of flowering time: interacting pathways
795 as a basis for diversity. *Plant Cell* **14 Suppl**, S111-130 (2002).
796 4. Aikawa S, Kobayashi MJ, Satake A, Shimizu KK, Kudoh H. Robust control of the
797 seasonal expression of the *Arabidopsis FLC* gene in a fluctuating environment. *Proc*
798 *Natl Acad Sci U S A* **107**, 11632-11637 (2010).
799 5. Song YH, Ito S, Imaizumi T. Flowering time regulation: photoperiod- and
800 temperature-sensing in leaves. *Trends Plant Sci* **18**, 575-583 (2013).
801 6. Golembeski GS, Imaizumi T. Photoperiodic regulation of florigen function in
802 *Arabidopsis thaliana*. *Arabidopsis Book* **13**, e0178 (2015).
803 7. Putterill J, Varkonyi-Gasic E. FT and florigen long-distance flowering control in
804 plants. *Curr Opin Plant Biol* **33**, 77-82 (2016).
805 8. Blümel M, Dally N, Jung C. Flowering time regulation in crops-what did we learn
806 from Arabidopsis? *Curr Opin Biotechnol* **32**, 121-129 (2015).
807 9. Kubota A, Kita S, Ishizaki K, Nishihama R, Yamato KT, Kohchi T. Co-option of a
808 photoperiodic growth-phase transition system during land plant evolution. *Nat*
809 *Commun* **5**, 3668 (2014).
810 10. Mockler T*, et al.* Regulation of photoperiodic flowering by *Arabidopsis*
811 photoreceptors. *Proc Natl Acad Sci U S A* **100**, 2140-2145 (2003).
812 11. Ratcliffe D. The geographical and ecological distribution of Arabidopsis and
813 comments on physiological variation. *Arabidopsis Information Service* **1 Suppl.**,
814 (1965).
815 12. Effmertova E. The behaviour of "summer annual", "mixed", and "winter annual"
816 natural populations as compared with early and late races in field conditions.
817 *Arabidopsis Information Service* **4**, (1967).

818 13. Thompson L. The spatiotemporal effects of nitrogen and litter on the population
819 dynamics of *Arabidopsis thaliana*. *J Ecol* **82**, 63-68 (1994).
820 14. Donohue K. Germination timing influences natural selection on life-history characters
821 in *Arabidopsis thaliana*. *Ecology* **83**, 1006-1016 (2002).
822 15. Griffith C, Kim E, Donohue K. Life-history variation and adaptation in the
823 historically mobile plant *Arabidopsis thaliana* (Brassicaceae) in North America. *Am J*
824 *Bot* **91**, 837-849 (2004).
825 16. Wilczek AM*, et al.* Effects of genetic perturbation on seasonal life history plasticity.
826 *Science* **323**, 930-934 (2009).
827 17. Picó FX. Demographic fate of *Arabidopsis thaliana* cohorts of autumn- and spring-
828 germinated plants along an altitudinal gradient. *J Ecol* **100**, 1009-1018 (2012).
829 18. Chiang GCK, Barua D, Dittmar E, Kramer EM, de Casas RR, Donohue K. Pleiotropy
830 in the wild: the dormancy gene *DOG1* exerts cascading control on life cycles.
831 *Evolution* **67**, 883-893 (2013).
832 19. Pruneda-Paz JL, Kay SA. An expanding universe of circadian networks in higher
833 plants. *Trends Plant Sci* **15**, 259-265 (2010).
834 20. Bieniawska Z, Espinoza C, Schlereth A, Sulpice R, Hincha DK, Hannah MA.
835 Disruption of the Arabidopsis circadian clock is responsible for extensive variation in
836 the cold-responsive transcriptome. *Plant Physiol* **147**, 263-279 (2008).
837 21. Imaizumi T, Tran HG, Swartz TE, Briggs WR, Kay SA. FKF1 is essential for
838 photoperiodic-specific light signalling in *Arabidopsis*. *Nature* **426**, 302-306 (2003).
839 22. Imaizumi T, Schultz TF, Harmon FG, Ho LA, Kay SA. FKF1 F-box protein mediates
840 cyclic degradation of a repressor of *CONSTANS* in *Arabidopsis*. *Science* **309**, 293-297
841 (2005).

842 23. Kinmonth-Schultz HA, *et al.* Cool night-time temperatures induce the expression of
843 *CONSTANS* and *FLOWERING LOCUS T* to regulate flowering in *Arabidopsis*. *New*
844 *Phytol* **211**, 208-224 (2016).
845 24. Yamaguchi A, Kobayashi Y, Goto K, Abe M, Araki T. *TWIN SISTER OF FT* (*TSF*)
846 acts as a floral pathway integrator redundantly with *FT*. *Plant Cell Physiol* **46**, 1175-
847 1189 (2005).
848 25. Krzymuski M, *et al.* The dynamics of *FLOWERING LOCUS T* expression encodes
849 long-day information. *Plant J* **83**, 952-961 (2015).
850 26. Mizoguchi T, *et al.* Distinct roles of *GIGANTEA* in promoting flowering and
851 regulating circadian rhythms in Arabidopsis. *Plant Cell* **17**, 2255-2270 (2005).
852 27. Amasino R. Seasonal and developmental timing of flowering. *Plant J* **61**, 1001-1013
853 (2010).
854 28. Holmes MG, Smith H. The function of phytochrome in plants growing in the natural
855 environment. *Nature* **254**, 512-514 (1975).
856 29. Wollenberg AC, Strasser B, Cerdan PD, Amasino RM. Acceleration of flowering
857 during shade avoidance in Arabidopsis alters the balance between *FLOWERING*
858 *LOCUS C*-mediated repression and photoperiodic induction of flowering. *Plant*
859 *Physiol* **148**, 1681-1694 (2008).
860 30. Kim SY, Yu X, Michaels SD. Regulation of *CONSTANS* and *FLOWERING LOCUS*
861 *T* expression in response to changing light quality. *Plant Physiol* **148**, 269-279 (2008).
862 31. Bouché F, Lobet G, Tocquin P, Périlleux C. FLOR-ID: an interactive database of
863 flowering-time gene networks in *Arabidopsis thaliana*. *Nucleic Acids Res* **44**, D1167-
864 1171 (2016).
865 32. Koornneef M, Alonso-Blanco C, Vreugdenhil D. Naturally occurring genetic
866 variation in *Arabidopsis thaliana*. *Annu Rev Plant Biol* **55**, 141-172 (2004).

867 33. Lee JH*, et al.* Regulation of temperature-responsive flowering by MADS-box
868 transcription factor repressors. *Science* **342**, 628-632 (2013).
869 34. Casal JJ, Candia AN, Sellaro R. Light perception and signalling by phytochrome A. *J*
870 *Exp Bot* **65**, 2835-2845 (2014).
871 35. Reed JW, Nagatani A, Elich TD, Fagan M, Chory J. Phytochrome A and
872 phytochrome B have overlapping but distinct functions in *Arabidopsis* development.
873 *Plant Physiol* **104**, 1139-1149 (1994).
874 36. Johnson E, Bradley M, Harberd NP, Whitelam GC. Photoresponses of light-grown
875 *phyA* mutants of *Arabidopsis* (Phytochrome A is required for the perception of
876 daylength extensions). *Plant Physiol* **105**, 141-149 (1994).
877 37. Yanovsky MJ, Kay SA. Molecular basis of seasonal time measurement in *Arabidopsis*.
878 *Nature* **419**, 308-312 (2002).
879 38. Genoud T*, et al.* FHY1 mediates nuclear import of the light-activated phytochrome A
880 photoreceptor. *PLoS Genet* **4**, e1000143 (2008).
881 39. Mockler TC, Guo H, Yang H, Duong H, Lin C. Antagonistic actions of *Arabidopsis*
882 cryptochromes and phytochrome B in the regulation of floral induction. *Development*
883 **126**, 2073-2082 (1999).
884 40. Valverde F, Mouradov A, Soppe W, Ravenscroft D, Samach A, Coupland G.
885 Photoreceptor regulation of CONSTANS protein in photoperiodic flowering. *Science*
886 **303**, 1003-1006 (2004).
887 41. Reed JW*, et al.* Independent action of ELF3 and phyB to control hypocotyl elongation
888 and flowering time. *Plant Physiol* **122**, 1149-1160 (2000).
889 42. Leivar P, Quail PH. PIFs: pivotal components in a cellular signaling hub. *Trends*
890 *Plant Sci* **16**, 19-28 (2011).

891 43. Nusinow DA, *et al.* The ELF4-ELF3-LUX complex links the circadian clock to
892 diurnal control of hypocotyl growth. *Nature* **475**, 398-402 (2011).
893 44. Jang S, *et al. Arabidopsis* COP1 shapes the temporal pattern of CO accumulation
894 conferring a photoperiodic flowering response. *EMBO J* **27**, 1277-1288 (2008).
895 45. Laubinger S, *et al. Arabidopsis* SPA proteins regulate photoperiodic flowering and
896 interact with the floral inducer CONSTANS to regulate its stability. *Development* **133**,
897 3213-3222 (2006).
898 46. Nakamichi N, *et al. Arabidopsis* clock-associated pseudo-response regulators PRR9,
899 PRR7 and PRR5 coordinately and positively regulate flowering time through the
900 canonical CONSTANS-dependent photoperiodic pathway. *Plant Cell Physiol* **48**,
901 822-832 (2007).
902 47. Park MJ, Kwon YJ, Gil KE, Park CM. LATE ELONGATED HYPOCOTYL
903 regulates photoperiodic flowering via the circadian clock in *Arabidopsis*. *BMC Plant*
904 *Biol* **16**, 114 (2016).
905 48. Lazaro A, Valverde F, Pineiro M, Jarillo JA. The *Arabidopsis* E3 ubiquitin ligase
906 HOS1 negatively regulates CONSTANS abundance in the photoperiodic control of
907 flowering. *Plant Cell* **24**, 982-999 (2012).
908 49. Huang H, *et al.* Identification of evening complex associated proteins in *Arabidopsis*
909 by affinity purification and mass spectrometry. *Mol Cell Proteomics* **15**, 201-217
910 (2016).
911 50. Schwartz CJ, Lee J, Amasino R. Variation in shade-induced flowering in *Arabidopsis*
912 *thaliana* results from *FLOWERING LOCUS T* allelic variation. *PLoS One* **12**,
913 e0187768 (2017).

914 51. Song YH, Smith RW, To BJ, Millar AJ, Imaizumi T. FKF1 conveys timing
915 information for CONSTANS stabilization in photoperiodic flowering. *Science* **336**,
916 1045-1049 (2012).
917 52. Yu JW*, et al.* COP1 and ELF3 control circadian function and photoperiodic flowering
918 by regulating GI stability. *Mol Cell* **32**, 617-630 (2008).
919 53. Sheerin DJ*, et al.* Light-activated phytochrome A and B interact with members of the
920 SPA family to promote photomorphogenesis in Arabidopsis by reorganizing the
921 COP1/SPA complex. *Plant Cell* **27**, 189-201 (2015).
922 54. Kim WY, Hicks KA, Somers DE. Independent roles for *EARLY FLOWERING 3* and
923 *ZEITLUPE* in the control of circadian timing, hypocotyl length, and flowering time.
924 *Plant Physiol* **139**, 1557-1569 (2005).
925 55. Rédei GP. Supervital mutants of Arabidopsis. *Genetics* **47**, 443-460 (1962).
926 56. Lin MK*, et al.* FLOWERING LOCUS T protein may act as the long-distance
927 florigenic signal in the cucurbits. *Plant Cell* **19**, 1488-1506 (2007).
928 57. Yoo SC*, et al.* Phloem long-distance delivery of FLOWERING LOCUS T (FT) to the
929 apex. *Plant J* **75**, 456-468 (2013).
930 58. Mitchell DE, Gadus MV, Madore MA. Patterns of assimilate production and
931 translocation in muskmelon (*Cucumis melo* L.) : I. diurnal patterns. *Plant Physiol* **99**,
932 959-965 (1992).
933 59. Savage JA, Zwieniecki MA, Holbrook NM. Phloem transport velocity varies over
934 time and among vascular bundles during early cucumber seedling development. *Plant*
935 *Physiol* **163**, 1409-1418 (2013).
936 60. Yasunaga E, Yano T, Araki T, Setoyama S, Kitano M. Effect of environmental
937 condition on xylem and phloem transport of developing fruit. *IFAC Proc Vol* **46**, 297-
938 301 (2013).

939 61. Shim JS, Kubota A, Imaizumi T. Circadian clock and photoperiodic flowering in
940 Arabidopsis: CONSTANS Is a hub for signal integration. *Plant Physiol* **173**, 5-15
941 (2017).
942 62. Pittendrigh CS, Minis DH. The entrainment of circadian oscillations by light and their
943 role as photoperiodic clocks. *Am Nat*, 261-294 (1964).
944 63. Gattermann R*, et al.* Golden hamsters are nocturnal in captivity but diurnal in nature.
945 *Biol Lett* **4**, 253-255 (2008).
946 64. Daan S*, et al.* Lab mice in the field: unorthodox daily activity and effects of a
947 dysfunctional circadian clock allele. *J Biol Rhythms* **26**, 118-129 (2011).
948 65. Vanin S*, et al.* Unexpected features of *Drosophila* circadian behavioural rhythms
949 under natural conditions. *Nature* **484**, 371-375 (2012).
950 66. Montelli S*, et al. period* and *timeless* mRNA splicing profiles under natural
951 conditions in *Drosophila melanogaster*. *J Biol Rhythms* **30**, 217-227 (2015).
952 67. Shimizu KK, Kudoh H, Kobayashi MJ. Plant sexual reproduction during climate
953 change: gene function *in natura* studied by ecological and evolutionary systems
954 biology. *Ann Bot* **108**, 777-787 (2011).
955 68. Kudoh H. Molecular phenology in plants: *in natura* systems biology for the
956 comprehensive understanding of seasonal responses under natural environments. *New*
957 *Phytol* **210**, 399-412 (2016).
958 69. Jefferson RA, Kavanagh TA, Bevan MW. GUS fusions: beta-glucuronidase as a
959 sensitive and versatile gene fusion marker in higher plants. *EMBO J* **6**, 3901-3907
960 (1987).
961 70. Nelson DC, Lasswell J, Rogg LE, Cohen MA, Bartel B. *FKF1*, a clock-controlled
962 gene that regulates the transition to flowering in *Arabidopsis*. *Cell* **101**, 331-340
963 (2000).

964 71. Kotake T, Takada S, Nakahigashi K, Ohto M, Goto K. *Arabidopsis TERMINAL*
965 *FLOWER 2* gene encodes a heterochromatin protein 1 homolog and represses both
966 *FLOWERING LOCUS T* to regulate flowering time and several floral homeotic genes.
967 *Plant Cell Physiol* **44**, 555-564 (2003).
968 72. Takada S, Goto K. TERMINAL FLOWER2, an Arabidopsis homolog of
969 HETEROCHROMATIN PROTEIN1, counteracts the activation of *FLOWERING*
970 *LOCUS T* by constans in the vascular tissues of leaves to regulate flowering time.
971 *Plant Cell* **15**, 2856-2865 (2003).
972 73. Reed JW, Nagpal P, Poole DS, Furuya M, Chory J. Mutations in the gene for the
973 red/far-red light receptor phytochrome B alter cell elongation and physiological
974 responses throughout Arabidopsis development. *Plant Cell* **5**, 147-157 (1993).
975 74. Liu XL, Covington MF, Fankhauser C, Chory J, Wagner DR. *ELF3* encodes a
976 circadian clock-regulated nuclear protein that functions in an Arabidopsis *PHYB*
977 signal transduction pathway. *Plant Cell* **13**, 1293-1304 (2001).
978 75. Rosler J, Klein I, Zeidler M. *Arabidopsis fhl*/*fhy1* double mutant reveals a distinct
979 cytoplasmic action of phytochrome A. *Proc Natl Acad Sci U S A* **104**, 10737-10742
980 (2007).
981 76. McNellis TW, von Arnim AG, Araki T, Komeda Y, Misera S, Deng XW. Genetic and
982 molecular analysis of an allelic series of *cop1* mutants suggests functional roles for
983 the multiple protein domains. *Plant Cell* **6**, 487-500 (1994).
984 77. Laubinger S, Fittinghoff K, Hoecker U. The SPA quartet: a family of WD-repeat
985 proteins with a central role in suppression of photomorphogenesis in Arabidopsis.
986 *Plant Cell* **16**, 2293-2306 (2004).
987 78. Leivar P*, et al.* Multiple phytochrome-interacting bHLH transcription factors repress
988 premature seedling photomorphogenesis in darkness. *Curr Biol* **18**, 1815-1823 (2008).

79. Yanovsky MJ, Mazzella MA, Whitelam GC, Casal JJ. Resetting of the circadian clock by phytochromes and cryptochromes in *Arabidopsis*. *J Biol Rhythms* **16**, 523-530 (2001).
80. Yakir E, Hilman D, Kron I, Hassidim M, Melamed-Book N, Green RM. Posttranslational regulation of CIRCADIAN CLOCK ASSOCIATED1 in the circadian oscillator of Arabidopsis. *Plant Physiol* **150**, 844-857 (2009).
81. Nakamichi N, Kita M, Ito S, Yamashino T, Mizuno T. PSEUDO-RESPONSE REGULATORS, PRR9, PRR7 and PRR5, together play essential roles close to the circadian clock of *Arabidopsis thaliana*. *Plant Cell Physiol* **46**, 686-698 (2005).
82. Lee JH, Yoo SJ, Park SH, Hwang I, Lee JS, Ahn JH. Role of *SVP* in the control of flowering time by ambient temperature in *Arabidopsis*. *Genes Dev* **21**, 397-402 (2007).
83. Kubota A, *et al.* TCP4-dependent induction of *CONSTANS* transcription requires GIGANTEA in photoperiodic flowering in *Arabidopsis*. *PLoS Genet* **13**, e1006856 (2017).
84. Baudry A, *et al.* F-box proteins FKF1 and LKP2 act in concert with ZEITLUPE to control *Arabidopsis* clock progression. *Plant Cell* **22**, 606-622 (2010).
85. Bolger AM, Lohse M, Usadel B. Trimmomatic: a flexible trimmer for Illumina sequence data. *Bioinformatics* **30**, 2114-2120 (2014).
86. Robinson MD, McCarthy DJ, Smyth GK. edgeR: a Bioconductor package for differential expression analysis of digital gene expression data. *Bioinformatics* **26**, 139-140 (2010).
87. Benjamini Y, Hochberg Y. Controlling the false discovery rate: a practical and powerful approach to multiple testing. *J R Stat Soc Series B Stat Methodol* **57**, 289-300 (1995).

88. Huang da W, Sherman BT, Lempicki RA. Systematic and integrative analysis of large gene lists using DAVID bioinformatics resources. *Nat Protoc* **4**, 44-57 (2009).

89. Shinomura T, Nagatani A, Hanzawa H, Kubota M, Watanabe M, Furuya M. Action spectra for phytochrome A- and B-specific photoinduction of seed germination in *Arabidopsis thaliana*. *Proc Natl Acad Sci U S A* **93**, 8129-8133 (1996).

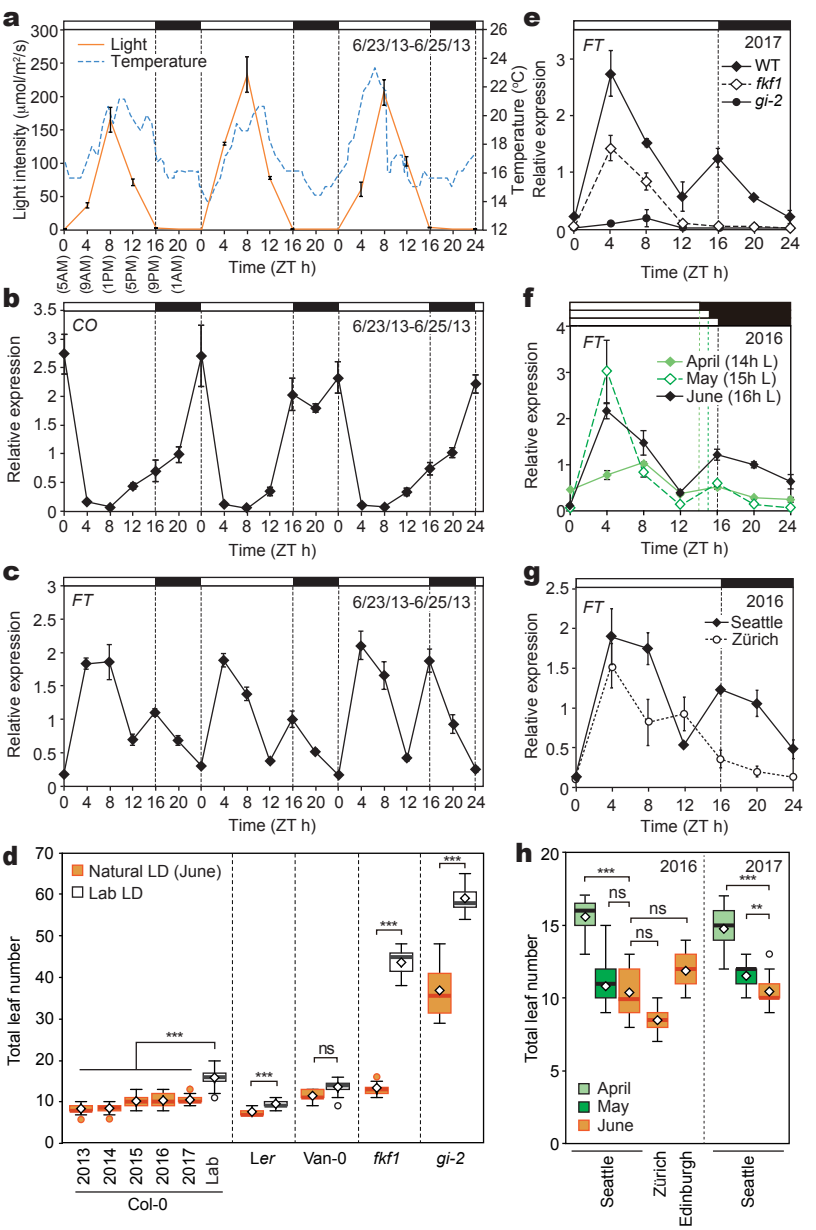
a
Light
Temperature
6/23/13-6/25/13
Light intensity (µmol/m²/s)
Temperature (°C)
(5AM) (9AM) (1PM) (5PM) (9PM) (1AM)
Time (ZT h)
b
CO
6/23/13-6/25/13
Relative expression
Time (ZT h)
c
FT
6/23/13-6/25/13
Relative expression
Time (ZT h)
d
Natural LD (June)
Lab LD
Total leaf number
2013
2014
2015
2016
2017
Lab
Col-0
Ler
Van-0
fkf1
gi-2
***
ns
e
FT
2017
WT
fkf1
gi-2
Relative expression
Time (ZT h)
f
FT
2016
April (14h L)
May (15h L)
June (16h L)
Relative expression
Time (ZT h)
g
FT
2016
Seattle
Zürich
Relative expression
Time (ZT h)
h
2016
2017
Total leaf number
April
May
June
Seattle
Zürich
Edinburgh
Seattle
***
ns
**

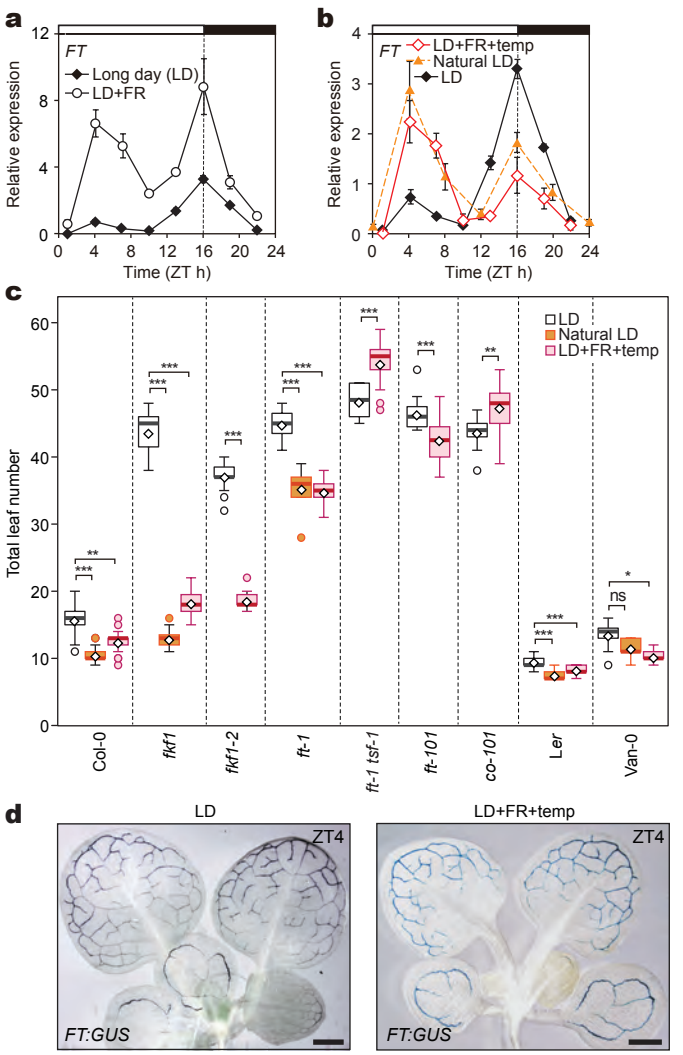
a
FT
Long day (LD)
LD+FR
Relative expression
Time (ZT h)
b
FT
LD+FR+temp
Natural LD
LD
Relative expression
Time (ZT h)
c
LD
Natural LD
LD+FR+temp
Total leaf number
Col-0
fkf1
fkf1-2
ft-1
ft-1 tsf-1
ft-101
co-101
Ler
Van-0
d
LD
LD+FR+temp
ZT4
ZT4
FT:GUS
FT:GUS

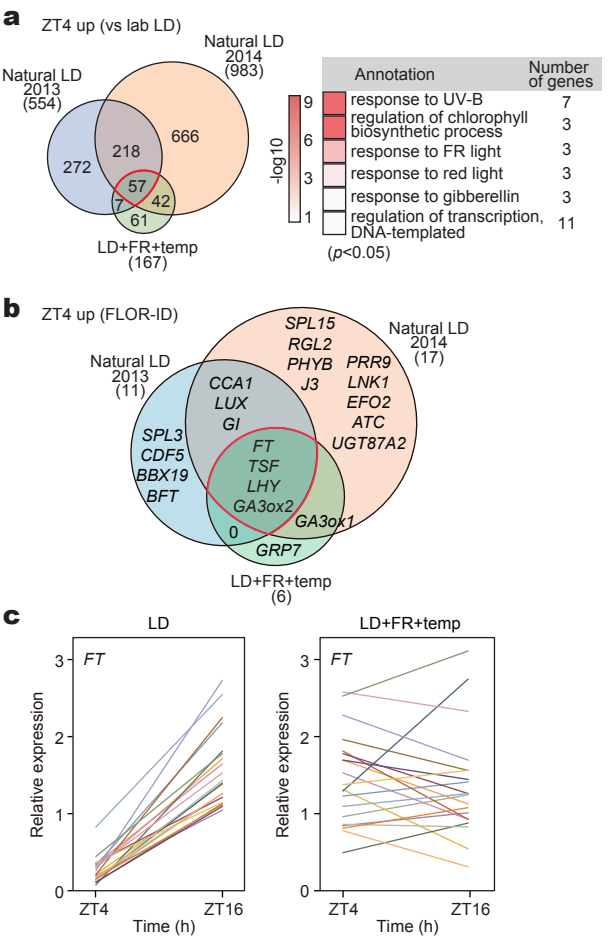
a
ZT4 up (vs lab LD)
Natural LD 2013 (554)
Natural LD 2014 (983)
LD+FR+temp (167)
272
218
666
57
7
42
61
-log10
9
6
3
1
Annotation
Number of genes
response to UV-B 7
regulation of chlorophyll biosynthetic process 3
response to FR light 3
response to red light 3
response to gibberellin 3
regulation of transcription, DNA-templated 11
(p<0.05)
b
ZT4 up (FLOR-ID)
Natural LD 2013 (11)
Natural LD 2014 (17)
LD+FR+temp (6)
SPL15
RGL2
PHYB
J3
PRR9
LNK1
EFO2
ATC
UGT87A2
CCA1
LUX
GI
SPL3
CDF5
BBX19
BFT
FT
TSF
LHY
GA3ox2
GA3ox1
0
GRP7
c
LD
LD+FR+temp
FT
Relative expression
Time (h)
ZT4
ZT16
0
1
2
3

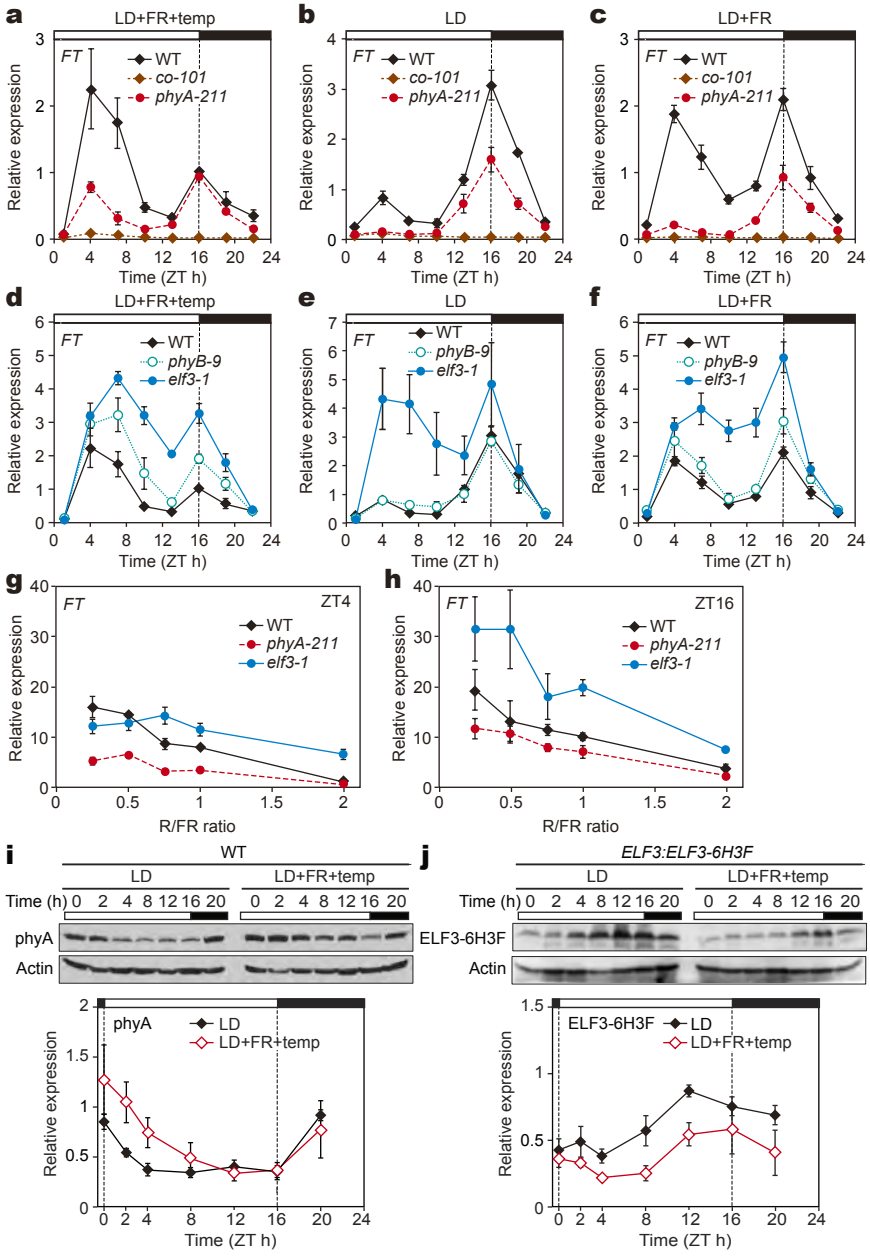
a
LD+FR+temp
FT
WT
co-101
phyA-211
Relative expression
Time (ZT h)
b
LD
c
LD+FR
d
phyB-9
elf3-1
e
f
g
ZT4
R/FR ratio
h
ZT16
i
WT
LD
LD+FR+temp
Time (h)
phyA
Actin
j
ELF3:ELF3-6H3F
ELF3-6H3F

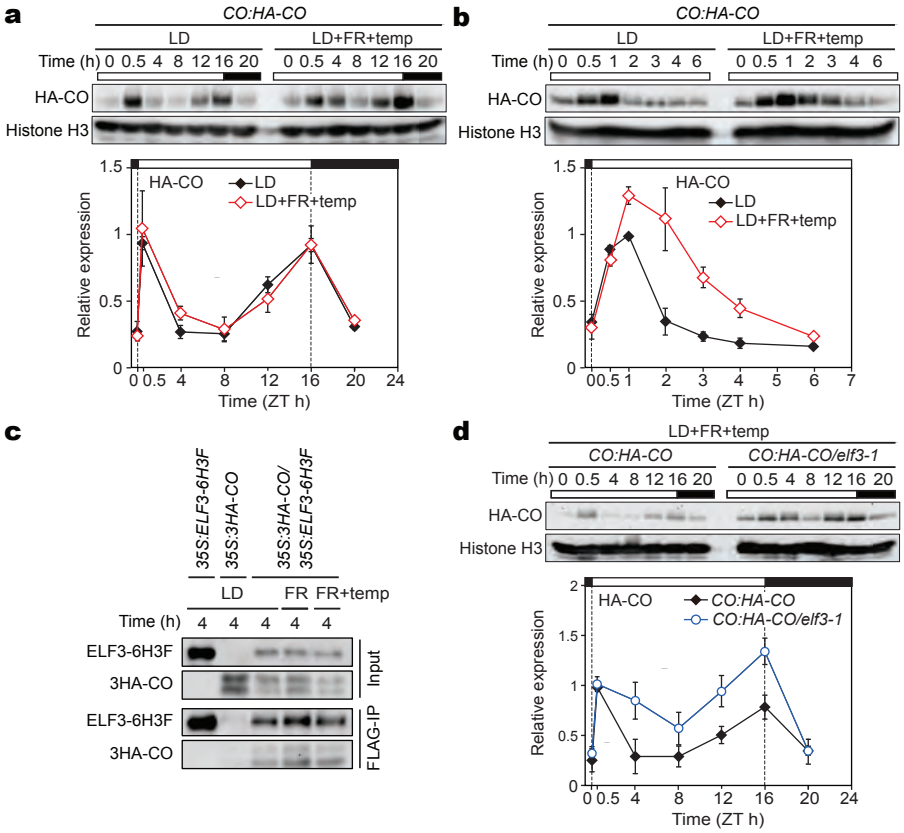
a
CO:HA-CO
LD
LD+FR+temp
Time (h) 0 0.5 4 8 12 16 20 0 0.5 4 8 12 16 20
HA-CO
Histone H3
HA-CO
LD
LD+FR+temp
Relative expression
Time (ZT h)
b
CO:HA-CO
LD
LD+FR+temp
Time (h) 0 0.5 1 2 3 4 6 0 0.5 1 2 3 4 6
HA-CO
Histone H3
HA-CO
LD
LD+FR+temp
Relative expression
Time (ZT h)
c
35S:ELF3-6H3F
35S:3HA-CO
35S:3HA-CO/
35S:ELF3-6H3F
LD
FR
FR+temp
Time (h) 4 4 4 4 4
ELF3-6H3F
3HA-CO
Input
ELF3-6H3F
3HA-CO
FLAG-IP
d
LD+FR+temp
CO:HA-CO
CO:HA-CO/elf3-1
Time (h) 0 0.5 4 8 12 16 20 0 0.5 4 8 12 16 20
HA-CO
Histone H3
HA-CO
CO:HA-CO
CO:HA-CO/elf3-1
Relative expression
Time (ZT h)
e
Lab LD
(R/FR ratio>2 and constant temperature)
CO protein
ELF3
phyA
FT mRNA
f
Natural LD
(R/FR ratio=1 and temperature oscillation)
CO protein
X
phyA
?
ELF3
Temperature
FT mRNA